Ricin A-Chain: Kinetic Isotope Effects and Transition State Structure with Stem-Loop RNA†

Xiang-Yang Chen,§ Paul J. Berti,‡ and Vern L. Schramm*

Contribution from the Department of Biochemistry, Albert Einstein College of Medicine, 1300 Morris Park Avenue, Bronx, New York 10461

Received August 2, 1999

Abstract: Ricin toxin A-chain (RTA) depurinates 28 S ribosomal RNA and small stem-loop RNAs at the first adenosine residue in a 5′-GAGA-3′ tetraloop. The transition state for depurination of stem-loop RNA by RTA was determined from kinetic isotope effects (KIEs). A stem-loop RNA, called A-10 (5′-GGCGAGAGCC-3′), was synthesized using isotopically labeled ATP. KIEs were measured for RNA substrates with adenylates containing [1′-^{14}C], [9-^{15}N], [1′-^{14}C,9-^{15}N], [7-^{15}N], [1′-^{3}H], [2′-^{3}H], [4′-^{3}H], or [5′-^{3}H]. Substrate-trapping experiments established that the Michaelis complex of RTA·[^{14}C]A-10 dissociates to free enzyme and [^{14}C]A-10 at least 20 times more frequently than its conversion to products, establishing minimal forward commitment to catalysis. KIEs were used to interpret the transition-state structure. The experimental KIEs differ from previous *N*-ribohydrolase chemistries. Large KIEs were measured for [1′-^{3}H] (1.163 ± 0.009) and [7-^{15}N] (0.981 ± 0.008). A modest isotope effect occurred with [9-^{15}N] (1.016 ± 0.005), and small KIEs were observed with [1′-^{14}C] (0.993 ± 0.004) and [2′-^{3}H] (1.012 ± 0.005). The experimental KIEs were analyzed using bond vibrational and quantum chemical approaches, which demonstrated that a complex is formed of RTA with the RNA ribooxocarbenium ion and adenine that is in equilibrium with the Michaelis complex. A slow, irreversible, and nonchemical step is followed by nucleophilic attack by water. Release of the depurinated A-10 and adenine products is rapid. Other *N*-ribohydrolases catalyze dissociative concerted A_ND_N (S_N2) transition states with weak participation of the leaving group and nucleophile. The KIEs for RTA establish a stepwise D_N*A_N mechanism and the existence of a cationic intermediate with a finite lifetime. The conformation of the ribosyl ring in the enzyme-stabilized RNA·ribooxocarbenium ion is 3′-endo, with an unusual dihedral angle of approximately 50° between C2′-H2′ and the vacant p-orbital of atom C1′. This conformation, which is unprecedented in *N*-ribohydrolases, is consistent with the geometry imposed by the stem-loop RNA backbone. These results establish that transition state analysis based on KIEs can be extended to the reactions of nucleic acid chemistry.

Introduction

Ricin is a potent cytotoxic A−B heterodimeric protein found in castor bean seeds.[1,2] The B-chain is a lectin that binds two or possibly more galactose residues of cell-surface glycolipids and glycoproteins.[3,4] Entry of ricin A-chain (RTA) into cells is facilitated by the lectin. The A-chain is released from the complex by reduction of a disulfide bond in the reducing environment of the cell cytoplasm.[5] One molecule of RTA is enough to inhibit protein biosynthesis in a cell and thereby kill it.[6] RTA catalyzes a specific adenine depurination of 28 S ribosomal RNA (rRNA) at nucleotide 4324 (Figure 1), destroying a binding site for eukaryotic elongation factors essential for protein synthesis. The toxin has a reported k_{cat} of 1777 min^{-1} on intact ribosomes, the source of its extreme toxicity.[6] The adenylate depurination site in rRNA has the sequence 5′-UCAGUACGAGAGGAACC-3′ in which the underlined A is predicted to be in a GAGA hairpin-tetraloop and is the site of depurination.[6−8] Short RNA stem-loop mimics of this sequence are poor substrates at neutral pH, with k_{cat} values $<10^{-5}$ that for intact isolated eukaryotic ribosomes.[7−10] However, a recent report established that short stem-loop RNAs are active substrates for RTA at low pH, with a pH optimum of 4.0.[11] Under

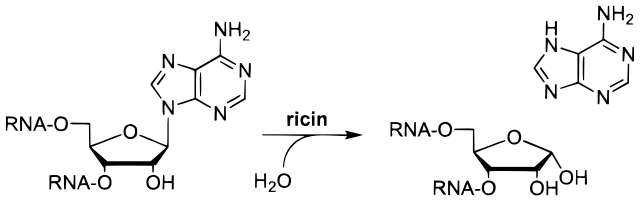

Figure 1. Depurination reaction catalyzed by ricin A-chain.

* To whom correspondence should be adressed. Tel.: (718) 430-2813. Fax: (718) 430-8565. E-mail: vern@aecom.yu.edu.

† Supported by NIH Research Grant CA72444.

‡ Present address: Department of Chemistry, McMaster University, Hamilton, Ontario, L8S 4M1, Canada.

§ Present address: Montsanto Company, MZ Q3A, St. Louis, MO 63167.

(1) Olsnes, S.; Pihl, A. In *Molecular Action of Toxins and Viruses*; Cohen, P., van Heyningen, S., Eds.; Elsevier Biomedical: New York, 1982; pp 51−105.

(2) Barbieri, L.; Battelli, M. G.; Stirpe, F. *Biochim. Biophys. Acta* **1993**, *1154*, 237−282.

(3) Frankel, A. E.; Burbage, C.; Tagge, E.; Chandler, J.; Willingham, M. C. *Biochemistry* **1996**, *35*, 14749−56.

(4) Venkatesh, Y. P.; Lambert, J. M. *Glycobiology* **1997**, *7*, 329−35.

(5) Thrush, G. R.; Lark, L. R.; Clinchy, B. C.; Vitetta, E. S. *Ann. Rev. Immunol*. **1996**, *14*, 49−71.

(6) Endo, Y.; Tsurugi, K. *J. Biol. Chem.* **1988**, *263*, 8735−8739.

(7) Endo, Y.; Chan, Y. L.; Lin, A.; Tsurugi, K.; Wool, I. G. *J. Biol. Chem.* **1988**, *263*, 7917−7920.

(8) Endo, Y.; Glück, A.; Wool, I. G. *J. Mol. Biol.* **1991**, *221*, 193−207.

(9) Chen, X.-Y.; Link, T. M.; Schramm, V. L. *J. Am. Chem. Soc.* **1996**, *118*, 3067−3068.

(10) Link, T. M.; Chen, X.-Y.; Niu, L. H.; Schramm, V. L. *Toxicon* **1996**, *34*, 1317−1324.

10.1021/ja992750i CCC: $19.00
Published on Web 02/10/2000

these conditions, the 10-mer sequence A-10 (5′-CGCGAGAGCG-3′) exhibited a k_{cat} of 4.1 ± 0.3 min^{-1} and a 14-mer sequence (5′-CGCGCGAGAGCGCG-3′) was the most efficient small stem-loop substrate, with a k_{cat} of 219 ± 14 min^{-1}. Both substrates had K_M values near 5 μM. These results suggested a general acid/base mechanism, in which protonation of an enzymatic acid (pK_a 4.0) is essential for catalysis.[11] It was proposed that the interaction of RTA with ribosomal protein or RNA increases the pK_a of the enzymatic acid toward neutrality. Finding conditions for maximal activity against small RNA permits more detailed mechanistic analysis of the reaction catalyzed by RTA. Our specific interest is to solve the transition-state structure for the reaction by the analysis of kinetic isotope effects (KIEs).

Catalysis by RTA has been proposed to proceed through an oxocarbenium-like transition state involving both ribosyl activation and leaving group protonation.[11] Kinetic and inhibition studies established that a stem-loop RNA analogue with iminoribitol replacing ribose at the depurination site binds to the enzyme with a K_i value of 0.18 μM.[11] It is now well established that the 1,4-dideoxyimino-ribitol group captures binding energy from enzymes with ribooxocarbenium character at the transition state.[12−16] In these cases, the structures of the transition state have been established from KIE analysis.

KIEs are defined as the ratio of rate constants for different isotopes of a given atom in a molecule, $^{light}k/^{heavy}k$. KIEs reflect the change in the vibrational environment between the reactant and the transition state of the reaction.[17] That is, they report on changes in the strength of the bonding forces in a molecule. For example, if a given bond becomes longer and weaker at the transition state than in the reactant, the decreased bond-stretching forces will lead to a looser vibrational environment and a normal KIE ($^{light}k/^{heavy}k > 1.0$). Conversely, an inverse KIE ($^{light}k/^{heavy}k < 1.0$) results from a bond becoming stronger at the transition state. Similarly, KIEs reflect changes in the forces controlling bond bending, torsions, and out-of-plane bending. Using substrate molecules isotopically labeled at multiple sites, KIEs can be measured and analyzed to give the transition-state structure in atomic detail.

In the present paper, analysis of KIEs established the transition-state structure of RNA depurination catalyzed by RTA. This transition state structure provides the first direct evidence for the chemical nature of an RNA depurination reaction. The results also provide guidelines for the design of transition-state inhibitors for RTA.

Materials and Methods

Materials. Ricin A-chain (RTA) was purchased from Inland Laboratories (Austin, TX). RNasin and calf intestinal phosphatase were obtained from Promega (Madison, WI). [U-^{14}C]Adenine was from Amersham (Piscataway, NJ). Methanol (^{13}C, 99%) was from Cambridge Isotope Laboratories (Andover, MA). T7 RNA polymerase was generously provided by Dr. Thomas Shrader of the Albert Einstein College of Medicine.

Synthesis of Isotopically Labeled ATP. Isotopically labeled ATP was prepared with specific incorporation of ^{3}H, ^{14}C, and ^{15}N from appropriately labeled glucose, ribose 5-phosphate, and adenine, according to published procedures.[18,19] In these methods, a series of enzymatic reactions are coupled to convert glucose, ribose and adenine to ATP. Yields of ATP in excess of 60% are obtained from labeled precursors. The labeled ATP was isolated and purified from the reaction mixture by C18 reversed-phase HPLC, eluting with 50 mM triethylammonium acetate (TEAA, pH 6.0) containing 5% methanol.

Synthesis of Isotopically Labeled Stem-Loop RNA 10-mer [A-10, (5′-GGCGAGAGCC-3′)]. In vitro transcription with T7 RNA polymerase was accomplished in reaction mixtures of 0.22 mM ATP, 4.5 mM GTP, 4.5 mM CTP, approximately 10^7 cpm each of appropriately ^{14}C- and ^{3}H-labeled ATPs, 0.2 μM DNA primer-template, 40 units RNasin, ca. 6400 units T7 RNA polymerase, 22 mM $MgCl_2$, 5 mM dithiothreitol (DTT), 1 mM spermidine, 0.01% triton X-100, 80 mg/mL PEG 8000, and 40 mM Tris·HCl (pH 8.1).[10,20] The primer and template strands of DNA were d(5′-TAATACGACTCACTATAG-3′) and d(5′-GGCTCTCGCCTATAGTGAGTCGTATTA-3′), respectively. After incubation at 37 °C overnight, 50 mM Na_2EDTA and 0.4 M NaOAc were added. The RNA was precipitated with 2.5 volumes of ethanol followed by cooling to −70 °C. Labeled A-10 RNA was isolated by 24% PAGE in 7 M urea, located by UV-shadowing, and eluted into 1 M NH_4OAc.[21] Purified RNA was desalted on a C18 Sep-Pak column (Waters, Milford, MA). Specific incorporation of the isotopically labeled ATP into A-10 RNA was demonstrated by RNA degradation to individual nucleosides, followed by HPLC analysis as described previously.[11]

Measurement of Kinetic Isotope Effects. The A-10 RNA used in reactions contained both ^{3}H- and ^{14}C-labels at the RTA depurination site. One isotopic label was at the position of interest for KIE measurement, and the other label was at a remote site.[22] Reaction mixtures buffered with 10 mM potassium citrate (pH 4.0) and 1 mM EDTA were divided into three portions. In the first portion, depurination was initiated by addition of 15 nM RTA and allowed to proceed to 20−30% completion at 37 °C. To the second portion, 1 μM RTA was added, and the reaction was continued for 2.5 h at 37 °C to give 100% hydrolysis. The third portion of the reaction mixture was incubated at 37 °C for 2.5 h in the absence of RTA as a control to detect any radioactive impurity and/or nonspecific hydrolysis of the N-ribosidic bond of the labeled RNA. All three reactions were stopped by addition of NaOH to 0.3 N, and the mixtures incubated at 37 °C overnight to convert intact RNA to nucleotides and depurinated RNA into nucleotides and ribose phosphates (from the depurination site). This treatment gives a mixture of ribose 2-phosphate and ribose 3-phosphate. The resulting mixtures were neutralized with 0.36 M HOAc. Each reaction mixture was divided into three equal portions, passed through three small columns of activated charcoal-cellulose (1:4 by weight), and eluted with 100 mM ribose in 100 mM potassium phosphate (pH 6.0).[18,22] Fractions of 1.0 mL were collected, and the radioactivity was counted to determine the ^{3}H/^{14}C ratio in the ribose phosphates. Labeled AMP from the second adenylate site in the GAGA tetraloop is retained on the charcoal columns. The observed KIEs were converted to experimental KIEs to correct for the isotopic depletion in the remaining substrate.[22]

Pulse-Chase Substrate Trapping Experiment. The commitment of enzyme-bound RNA to catalysis was measured by pulse-chase substrate trapping experiments.[23,24] The purpose of the experiment is to determine the fraction of enzyme-bound labeled A-10 ([^{14}C]A-10) converted to product in the first turnover following dilution with excess

(11) Chen, X.-Y.; Link, T. M.; Schramm, V. L. *Biochemistry* **1998**, *37*, 11605−11613.
(12) Horenstein, B. A.; Schramm, V. L. *Biochemistry* **1993**, *32*, 9917−25.
(13) Horenstein, B. A.; Zabinski, R. F.; Schramm, V. L. *Tetrahedron Lett.* **1993**, *34*, 7213−7216.
(14) Boutellier, M.; Horenstein, B. A.; Semenyaka, A.; Schramm, V. L.; Ganem, B. *Biochemistry* **1994**, *33*, 3994−4000.
(15) Parkin, D. W.; Limberg, G.; Tyler, P. C.; Furneaux, R. H.; Chen, X.-Y.; Schramm, V. L. *Biochemistry* **1997**, *36*, 3528−3534.
(16) Furneaux, R. H.; Limberg, G.; Tyler, P. C.; Schramm, V. L. *Tetrahedron* **1997**, *53*, 2915−2930.
(17) Huskey, W. P. In *Enzyme Mechanism from Isotope Effects*; Cook, P. F., Ed.; CRC Press: Boca Raton, FL, 1991; pp 37−72.
(18) Parkin, D. W.; Leung, H. B.; Schramm, V. L. *J. Biol. Chem.* **1984**, *259*, 9411−9417.
(19) Rising, K. A.; Schramm, V. L. *J. Am. Chem. Soc.* **1994**, *116*, 6531−6536.
(20) Milligan, J. F.; Groebe, D. R.; Witherell, G. W.; Uhlenbeck, O. C. *Nucleic Acids Res.* **1987**, *15*, 8783−8798
(21) Damha, M. J.; Ogilvie, K. K. In *Protocols for Oligonucleotides and Analogues: Synthesis and Properties*; Agrawal, S., Ed.; Methods in Molecular Biology 20; Humana Press: Totowa, NJ, 1993; pp 81−114.
(22) Parkin, D. W. In *Enzyme Mechanism from Isotope Effects*; Cook, P. F., Ed.; CRC Press: Boca Raton, FL, 1991; pp 269−290.

unlabeled A-10. In the equation

$$E + [^{14}C]A\text{-}10 \underset{}{\overset{k_{-1}}{\leftarrow}} E\cdot[^{14}C]A\text{-}10 \overset{k_2}{\rightarrow} E + \text{products}$$

the ratio for k_2/k_{-1} is established by the relative amounts of [^{14}C]A-10 that appears in products and substrate following the dilution step and several catalytic turnovers. RTA (30 μM) was rapidly mixed with 50 μM [5′-^{14}C]A-10 (^{14}C-labeled at the 5′-carbon in both adenosine residues, 1.0×10^5 cpm) in 10 mM potassium citrate (pH 4.0) and 1 mM EDTA and incubated for 6 s at 37 °C. These conditions generate the Michaelis complex at a concentration of 25 μM, with an incubation time to permit less than a single catalytic turnover. The reaction was either terminated immediately by the addition of 0.3 M NaOH or the mixture was diluted with 100-fold molar excess of unlabeled A-10 and the reaction was allowed to continue. Following dilution with unlabeled A-10, aliquots from the reaction mixture were removed periodically over the next 60 s and the reactions stopped with 0.3 M NaOH. Samples were incubated at 37 °C overnight to degrade the RNAs. The resulting mixtures were neutralized with 0.36 M HOAc and then passed through columns of activated charcoal-cellulose (1:4 by weight), eluted with 100 mM ribose in 100 mM potassium phosphate (pH 6.0). Fractions of eluent (1 mL) were collected and counted for [5-^{14}C]ribose phosphate. The radioactivity was used to determine the extent of hydrolysis before and after dilution with unlabeled A-10.

Hydrolysis of Stem-Loop RNA in the Presence of Free Adenine. To 50 μL reaction mixtures containing 20 μM A-10, 5 μCi [U-^{14}C]-adenine, 2 mM unlabeled adenine, 1 mM EDTA, and 10 mM potassium citrate (pH 4.0) was added 0.03 or 1 μM RTA. After incubation at 37 °C for 2 h, the mixtures were extracted three times with *n*-BuOH, and NaOH was added to 0.3 M before heating at 55 °C for 1.5 h. The resulting hydrolysate was neutralized with 0.36 M HOAc, diluted with an equal volume of buffer containing 0.1 M Tris·HCl (pH 9.3), 2 mM $MgCl_2$, 0.2 mM $Zn(OAc)_2$, and 2 mM spermidine, and treated with 5 U of calf intestinal phosphatase at 37 °C for an additional 2 h. Adenosine was separated by C18 reversed-phase analytical column with isocratic elution in 50 mM NH_4OAc (pH 5.0) containing 10% methanol, at a flow rate of 1 mL/min. The adenosine peak was detected by absorbance at 260 nm, collected, and analyzed for radioactivity.

Hydrolysis of Stem-Loop RNA in the Presence of Methanol. RTA (1 μM) was added to a 10 mL reaction mixture containing 100 μM A-10 and 2 mL ^{13}C-methanol buffered with 10 mM potassium citrate (pH 4.0) and 1 mM EDTA. The reaction was incubated at 37 °C overnight with another 1 μM of RTA added after 6 h. The mixture was extracted three times with phenol/chloroform/isoamyl alcohol (pH 6.7) to remove the protein and then lyophilized. The resulting sample was dissolved in 0.6 mL of water containing 10% D_2O and analyzed by ^{13}C NMR on a Bruker DRX-300 spectrometer. No peak corresponding to the methyl group of a methylriboside residue was observed.

Transition-State Modeling. All structure optimizations and energy and frequency calculations were performed using the GAUSSIAN 94 suite of programs,[25] using hybrid density functional theory with Becke's exchange functional[26] and Perdew and Wang's correlation functional,[27] with the 6-31+G** basis set (RB3PW91/6-31+G**), except as noted below. Harmonic frequencies were scaled by 0.956.[28] Fractionation factors were calculated using QUIVER,[29] with the Cartesian force constants scaled by 0.9139 (= 0.956^2). Equilibrium isotope effects (EIEs) were calculated from the fractionation factors as EIE = $\phi_{\text{initial}}/\phi_{\text{final}}$. In calculations on hypothetical ion·neutral complexes, bond order vibrational analysis was performed using the program VIBIE[30] with force constants selected to match the ab initio calculated EIEs for reactions **1** ↔ **2** + **5** (Figure 2). The molecular structure was interpolated between **1** and **2** + **5** using the structure interpolation approach described previously.[31]

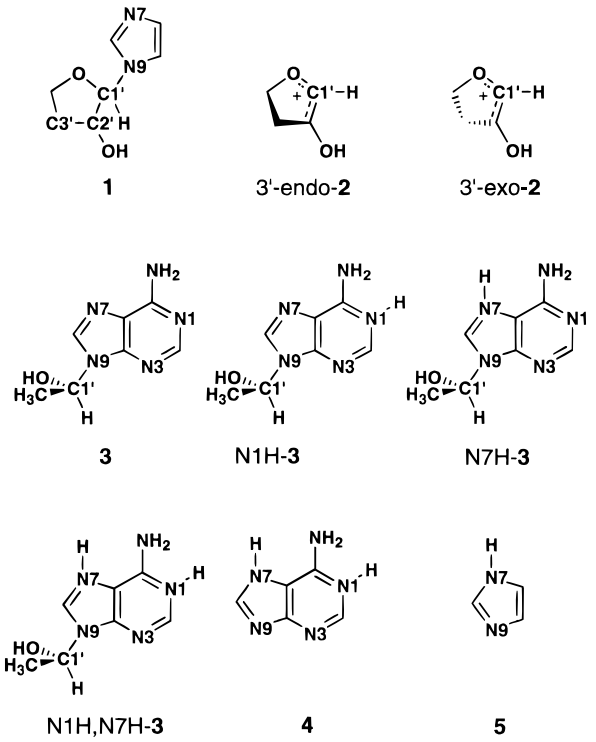

Figure 2. Molecules used in the ab initio analysis for equilibrium and kinetic isotope effects for formation of ribooxocarbenium ions and related transition-state or equilibrium species. Atoms are numbered as they would be at analogous positions in the RNA substrate molecule. *Z*-matrixes of the optimized structures are available in the Supporting Information.

To determine the effect of adenine ring protonation on the energetics of C−N bond breakage, the C1′−N9 bond of compound **3** in different protonation states was fixed at different lengths and the rest of the molecule re-optimized, and then the energies were calculated. This was done at the RB3PW91/6-31+G**//RHF/3-21G** level, except that some calculations were also done at the RB3PW91/6-31+G**// RB3PW91/6-31+G** level. Zero point energy corrections were not used because these molecules were not at a stationary point.

Results

Synthesis of Isotopically Labeled RNA. A-10 stem-loop RNA molecules containing isotopically labeled adenosine residues (Figure 3) were synthesized by in vitro transcription using primer-directed T7 RNA polymerase (Figure 4). The yield was over 40% on the basis of incorporation of radiolabeled ATP precursors. The RNA product has a triphosphate group at its 5′-terminus that can be removed by treatment with alkaline phosphatase. The 1′-^{3}H KIEs from A-10 stem-loop RNAs were measured with and without the triphosphate group. There were no significant differences in the KIE, and all subsequent KIE measurements were performed on RNA without 5′-dephosphorylation.

(23) Rose, I. A. *Methods Enzymol.* **1995**, *249*, 315−340.
(24) Markham, G. D.; Parkin, D. W.; Mentch, F.; Schramm, V. L. *J. Biol. Chem.* **1987**, *262*, 5609−5615.
(25) Frisch, M. J.; Trucks, G. W.; Schlegel, H. B.; Gill, P. M. W.; Johnson, B. G.; Robb, M. A.; Cheeseman, J. R.; Keith, T.; Petersson, G. A.; Montgomery, J. A.; Raghavachari, K.; Al-Laham, M. A.; Zakrzewski, V. G.; Ortiz, J. V.; Foresman, J. B.; Cioslowski, J.; Stefanov, B. B.; Nanayakkara, A.; Challacombe, M.; Peng, C. Y.; Ayala, P. Y.; Chen, W.; Wong, M. W.; Andres, J. L.; Replogle, E. S.; Gomperts, R.; Martin, R. L.; Fox, D. J.; Binkley, J. S.; Defrees, D. J.; Baker, J.; Stewart, J. P.; Head-Gordon, M.; Gonzalez, C.; Pople, J. A. *Gaussian 94, Revision C.2, D.4*; Gaussian, Inc.: Pittsburgh, PA, 1995.
(26) Becke, A. D. *Phys. Rev. A* **1988**, *38*, 3098−3100.
(27) Perdew, J. P.; Wang, Y. *Phys. Rev. B* **1992**, *45*, 13244.
(28) Wong, M. W. *Chem. Phys. Lett.* **1996**, *256*, 391−399.
(29) Saunders: M.; Laidig, K. E.; Wolfsberg, M. *J. Am. Chem. Soc.* **1989**, *111*, 8989−8994.
(30) Huskey, W. P. *J. Am. Chem. Soc.* **1996**, *118*, 1663−1668.
(31) Berti, P. J.; Schramm, V. L. *J. Am. Chem. Soc.* **1997**, *119*, 12069−12078.

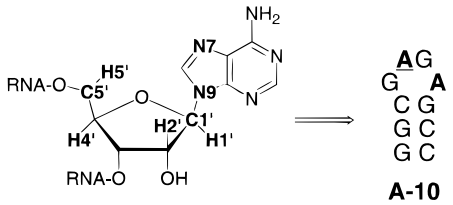

Figure 3. Stem-loop RNA 10-mer (A-10) with labeled adenosine residues. The atomic positions shown in bold were individually or multiply labeled with ^{3}H, ^{14}C, or ^{15}N for KIE measurements. The underlined A in A-10 is the RTA depurination site.

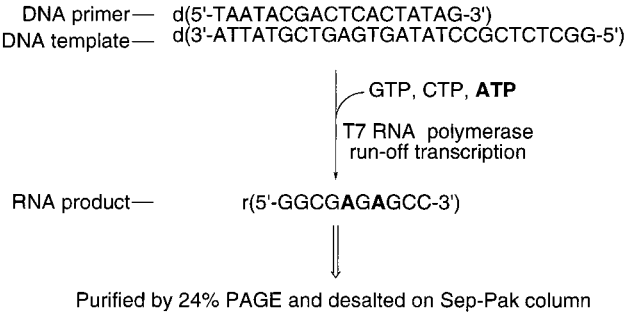

Figure 4. Synthesis of A-10 stem-loop RNA with labeled adenylates. Synthesis was accomplished by T7 RNA polymerase with the indicated DNA primer-template strands and nucleotide triphosphates. Labeled ATP was added as indicated in the text with the isotopic labels summarized in Table 1. Template-directed polymerization of RNA by T7 RNA polymerase begins by binding an unencoded GTP which leaves the completed strand with a 5′-GTP residue.

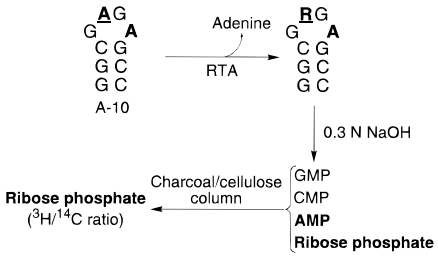

Figure 5. Protocol for the measurement of KIEs using the competitive radiolabel method. A mixture of A-10 RNAs with ^{3}H, ^{14}C, or ^{15}N at the depurination site is used as substrate. Using [1′-^{3}H]A and [5′-^{14}C]A A-10, for example, provides the [1′-^{3}H] KIE. Depurination gives an RNA molecule with a ribose-containing site (**R**). Hydrolysis in 0.3 M NaOH yields a mixture of ribose 2- and 3-phosphate from the RTA depurination site and nucleotide 2′- and 3′-phosphates from the other sites. Ribose phosphate elutes quantitatively from charcoal, while all nucleotides and bases are retained.

Kinetic Isotope Effect Measurement. Experimental KIEs were determined by measurement of the $^{3}H/^{14}C$ ratio in the ribosyl group at the abasic site of the depurinated RNA product following RNA degradation (Figure 5). A single reaction mixture was divided into two samples and hydrolyzed with RTA to 20−30% completion in one sample and 100% completion in the second. After depurination, the reactions were stopped, and the mixture of RNAs and adenine-depurinated RNAs was chemically degraded in 0.3 M NaOH.[32] RNAs were cleanly converted to ribonucleotides (the mixed 2′- and 3′-monophosphates of adenosine, guanosine and cytidine) at all sites except the depurination site. Ribose phosphate was formed only from the depurination site. Charcoal columns rigorously separate unreacted AMPs from ribose phosphates. Measurement of $^{3}H/^{14}C$ in the ribose phosphates by scintillation counting gives the KIE. Control experiments established that no ribose or ribose phosphate were formed in the absence of RTA. Complete depurination of RNA and its 100% conversion to ribose phosphate, AMP, GMP, and CMP was confirmed in parallel analyses by HPLC and quantitation of label in the AMP and ribose phosphate fractions. The experimental KIEs for RNA depurination catalyzed by RTA are summarized in Table 1.

(32) Adams, R. L. P.; Burdon, R. H.; Campbell, A. M.; Smellie, R. M. S. *The Biochemistry of Nucleic Acids*, 8th ed.; Academic Press: New York: 1976; pp.69−71.

Table 1. Kinetic Isotope Effects from RNA Depurination Catalyzed by Ricin A-Chain

RNA 10-mer	type of KIE	experimental KIEs[a]
[1′-^{14}C],[5′-^{3}H]	primary ^{14}C	0.993 ± 0.004 (3)[b]
[9-^{15}N, 5′-^{14}C],[5′-^{3}H]	primary ^{15}N	1.016 ± 0.005 (3)[b]
[9-^{15}N, 1′-^{14}C],[5′-^{3}H]	combined $^{15}N + ^{14}C$	1.012 ± 0.004 (4)[b]
[7-^{15}N, 5′-^{14}C],[5′-^{3}H]	secondary ^{15}N	0.981 ± 0.008 (2)[b]
[1′-^{3}H],[5′-^{14}C]	α-secondary ^{3}H	1.163 ± 0.009 (6)
[2′-^{3}H],[5′-^{14}C]	β-secondary ^{3}H	1.012 ± 0.005 (5)
[4′-^{3}H],[5′-^{14}C]	γ-secondary ^{3}H	0.992 ± 0.004 (3)
[5′-^{3}H],[5′-^{14}C]	δ-secondary ^{3}H	0.996 ± 0.003 (4)

[a] The number in parentheses is the number of independent KIE experiments. Each independent reaction was analyzed in triplicate. [b] KIEs were corrected for the 5′-^{3}H KIE according to the expression: $KIE_{experimental} = KIE_{observed}$(5′-^{3}H KIE).

Commitment to Catalysis. Forward commitment to catalysis is the probability that substrate in the Michaelis complex will be converted to product, relative to being released as unchanged substrate. Because significant forward commitment would suppress the intrinsic KIEs, it was measured directly by substrate trapping experiments. A large excess of unlabeled A-10 was added to a reaction mixture containing ^{14}C labeled A-10 in a Michaelis complex with RTA. If the commitment to catalysis is negligible, addition of unlabeled A-10 would result in displacement of labeled A-10 from the Michaelis complex. Labeled product formed during the "chase" phase of the experiment would extrapolate back to the amount present when the unlabeled A-10 was added (Figure 6). Within the ±5% error of the experiment, all of the enzyme-bound RNA was released from the enzyme and equilibrated with the excess unlabeled RNA before it was converted to products. The forward commitment factor is therefore less than 5%. Hydrolysis of the glycosidic bond from the enzyme−substrate complex is therefore slow compared to dissociation of the complex. A 5% commitment to catalysis would result in insignificant corrections to the experimental KIEs.

Reverse commitment to catalysis was also assessed by partial RTA-depurination of unlabeled stem-loop RNA in the presence of [U-^{14}C]adenine and quantitating the formation of labeled stem-loop RNA. There was no detectable label in the residual RNA, consistent with an irreversible step following adenine formation and negligible reverse commitment to catalysis (data not shown).

Depurination in the Presence of Methanol. The depurination reaction was performed in buffer containing 20% ^{13}C-methanol for two purposes: to probe the solvent accessibility of the enzyme active site during catalysis and, if methyl-riboside was formed, to determine the stereochemistry of the reaction. There was significant RTA inactivation by methanol during the overnight reaction, so more enzyme was added after 6 h incubation. The reaction went 50% to completion. There was no detectable formation of the methyl-riboside-containing RNA product. Given the high ^{13}C enrichment in the solvent methanol, product containing less than 5% of methyl riboside would have been detected.

The Kinetic Isotope Effects. A near-unity primary 1′-^{14}C KIE was observed, suggesting that the depurination involves a

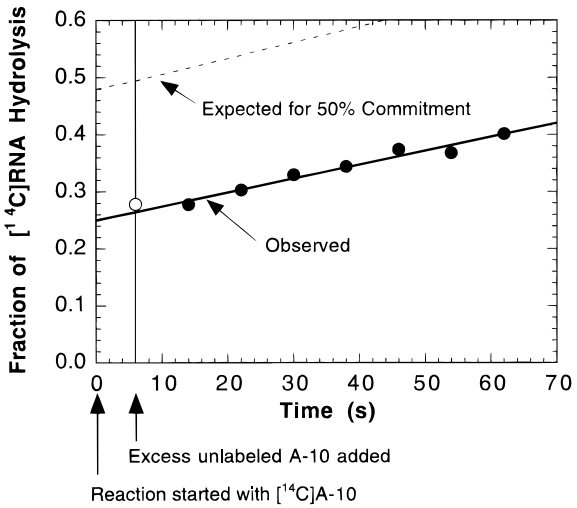

Figure 6. Commitment to catalysis for depurination of A-10 RNA by RTA. RTA was mixed with [5′-^{14}C]-labeled A-10 RNA. After 6 s, the reaction was either terminated and analyzed for product formation (○) or diluted with chase solution containing a large excess of unlabeled A-10 RNA. Aliquots were removed at the indicated time points and analyzed for product formation (●). Labeled product continues to be formed during the chase part of the experiment from the pool of substrate that is now highly diluted by unlabeled A-10. If there is no significant commitment to catalysis, the labeled A-10 in the Michaelis complex will be displaced by the unlabeled A-10. In this case, the amount of labeled product formed during the chase part of the experiment will extrapolate back to the amount present when the chase solution was added. If there is significant commitment to catalysis, the amount of labeled product formed will be higher, displaced upward by the amount of labeled A-10 that did not dissociate from the Michaelis complex with the enzyme before catalysis. The expected result for 50% commitment to catalysis is shown for comparison (- - -).

D_N*A_N-like[33] (S_N1) stepwise mechanism with leaving group departure and nucleophile approach occurring in separate steps (Figure 7). The primary 9-^{15}N KIE of 1.016 is less than the value of 1.024 expected for a fully broken C−N bond (Table 2). The inverse 7-^{15}N KIE (0.981) is consistent with protonation at the transition state. The negative charge that would form on N9 upon breaking the C1′−N9 bond can be neutralized by protonation at N7 and delocalization of the charge by resonance stabilization through the five-membered ring of the adenine. Protonation would increase the vibrational stiffness at N7, resulting in an inverse KIE. The relatively large α-secondary 1′-^{3}H KIE of 1.163 is consistent with a transition state having oxocarbenium ion character with sp^2-hybridization at the anomeric carbon. Rehybridization from sp^3 to sp^2 at C1′ increases the out-of-plane bending motion of H1′. The *β*-secondary 2′-^{3}H KIE of 1.012 is a uniquely small value for *N*-ribosyl hydrolases. A large *β*-secondary KIE is typically associated with strong hyperconjugation between the elongating glycosidic bond and the C2′−H2′ bond of an oxocarbenium ion-like transition state.[34,35] Hyperconjugation requires orbital overlap between the empty p-orbital of C1′ and the *π*-symmetry orbital of C2′;[34,35] therefore, it depends on the p-orbital−C1′−C2′−H2′ dihedral angle. The small *β*-secondary KIE suggests a large dihedral angle between the p-orbital of C1′ and the C2′−H2′ bond, which is consistent with an oxocarbenium ion in a 3′-endo conformation.[36]

The remote 5′-^{3}H KIE of 0.996 stands in contrast to the large, normal 5′-^{3}H KIEs observed in other enzyme-catalyzed *N*-riboside hydrolysis reactions, ranging from 1.006 to 1.051.[37−39] These remote KIEs can result from distortion of the O5′−C5′−C4′ bond angle and/or protonation of the adjacent phosphate residue in nucleotides. At the transition state for RTA-catalyzed RNA hydrolysis, there is little change in this portion of the substrate.

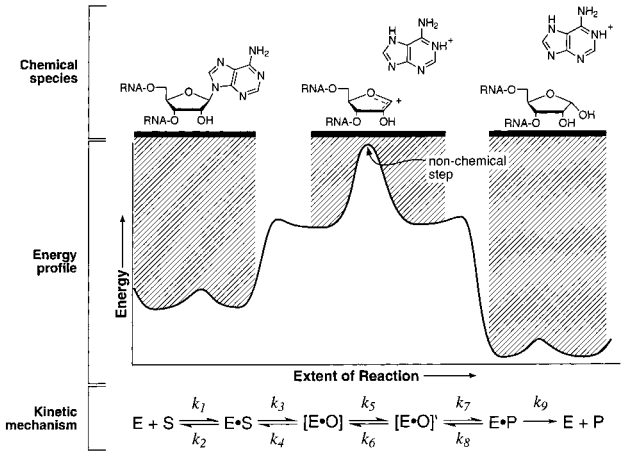

Figure 7. Proposed mechanism of RTA-catalyzed A-10 RNA hydrolysis. Free RTA (E) and RNA substrate (S) combine to form a Michaelis complex (E·S), which then proceeds to form a noncovalent RTA·(oxocarbenium ion + adenine) complex (E·O). (E + S) and (E·O) are in equilibrium, with $k_4 \gg k_5$. An irreversible step (i.e., $k_6 \ll k_7$) then occurs that is rate-limited by a nonchemical process to yield (E·O)′. The nature of (E·O)′ is not known; it will depend on the nature of the nonchemical step k_5 (see text). (E·O)′ then undergoes nucleophilic attack to form the RTA·(depurinated RNA + adenine) complex (E·P), which dissociates in the last step to form free RTA and products (E + P). The ordinate of the energy profile is strictly a qualitative illustration of the proposed mechanism, with no quantitative units.

Table 2. Calculated Fractionation Factors and Equilibrium Isotope Effects.

	fractionation factors (*ϕ*)					
isotopic label	**1**	**3**	3-*endo*-**2**	**4**	EIE[a]	exptl KIE
1′-^{14}C	1.315		1.306		1.007	0.993
9-^{15}N		1.119		1.094	1.024	1.016
7-^{15}N		1.092		1.107	0.985	0.981
1′-^{3}H	31.128		24.172		1.288	1.163
2′-^{3}H	29.486		29.666		0.994	1.012

[a] EIE = ϕ**1**/ϕ**2** or ϕ**3**/ϕ**4**, as described in the Materials and Methods.

Discussion

Proposed Mechanism. RTA-catalyzed RNA hydrolysis is proposed to proceed through a stepwise mechanism with equilibrium formation of a ribooxocarbenium ion intermediate complexed with the enzyme, followed by an isotopically

(33) Guthrie, R. D.; Jencks, W. P. *Acc. Chem. Res.* **1989**, *22*, 343−349. In the IUPAC nomenclature, a reaction mechanism is divided into elementary steps, with D_N representing a nucleophilic dissociation and A_N representing a nucleophilic addition. The asterisk indicates that the reaction is stepwise, with a discrete intermediate formed between leaving group departure and nucleophile approach. The asterisk (as distinct from "+") also indicates that the intermediate is too short-lived to diffusionally separate from the leaving group. A bimolecular (S_N2) reaction would be represented as A_ND_N.

(34) Hehre, W. J. *Acc. Chem. Res.* **1975**, *8*, 369−376.

(35) Sunko, D. E.; Szele, I.; Hehre, W. J. *J. Am. Chem. Soc.* **1977**, *99*, 5000−5004.

(36) Altona, C.; Sundaralingam, M. *J. Am. Chem. Soc.* **1972**, *94*, 8205−8211.

(37) Horenstein, B. A.; Parkin, D. W.; Estupinan, B.; Schramm, V. L. *Biochemistry* **1991**, *30*, 10788−10795.

(38) Mentch, F.; Parkin, D. W.; Schramm, V. L. *Biochemistry* **1987**, *26*, 921−930. Parkin, D. W.; Mentch, F.; Banks, G. A.; Horenstein, B. A.; Schramm, V. L. *Biochemistry* **1991**, *30*, 4586−4594.

(39) Kline, P. C.; Schramm, V. L. *Biochemistry* **1993**, *32*, 13212−13219.

insensitive, irreversible step leading to product formation (Figure 7). The most important experimental KIE for determining the transition state was the primary 1′-^{14}C KIE, which was inverse. KIEs calculated both by bond order vibrational analysis (BOVA)[40] and ab intio quantum mechanical methods indicate that the smallest 1′-^{14}C KIE possible for an A_ND_N mechanism is 1.025 (BOVA) to 1.029 (ab initio), even for highly dissociative transition states. The smallest experimental 1′-^{14}C KIE previously determined in this laboratory for an adenylate substrate was 1.032.[41] The large calculated 1′-^{14}C KIEs are due in part to the reaction coordinate itself. Simultaneous departure of the leaving group and approach of the nucleophile makes a contribution to the 1′-^{14}C KIE of > 1.01. For D_N*A_N or $D_N + A_N$ stepwise mechanisms, the reaction coordinate contribution is smaller because it includes only one of the leaving group or the nucleophile. Nonetheless, the ab initio calculated KIEs of 1.010 to 1.018 for stepwise mechanisms[42] are not inverse and are larger than the experimental 1′-^{14}C KIE. Thus, the 1′-^{14}C KIE was inconsistent with traditional concerted or stepwise mechanisms for nucleophilic substitution. It was consistent, however, with the calculated *equilibrium* isotope effect for formation of an oxocarbenium ion intermediate.

The first chemical step is equilibrium formation of a discrete, stable complex of the enzyme with the oxocarbenium ion and N7-protonated adenine base (E·O in Figure 7) that can freely revert back to the reactant RNA (i.e., $k_4 \gg k_5$). The "stable" oxocarbenium ion has a lifetime of at least several bond vibrations ($>10^{-12}$ s), but this mechanism places no upper limit on its lifetime other than that of k_{cat}. The precise nature of the following step (k_5) is unknown. To be consistent with the experimental KIEs, it must be essentially irreversible ($k_6 \ll k_7$) and isotopically insenstive (i.e., the intrinsic KIE on step k_5, α_5, is 1). Step k_5 may be a conformational change of the protein or simply diffusion of water into position to perform nucleophilic attack on the oxocarbenium ion (see below). Species (E·O)′ could be a complex of the enzyme in an altered conformation with the oxocarbenium ion, or the enzyme·oxocarbenium ion complex with water poised for nucleophilic attack. Given the fact that an oxocarbenium ion is too reactive to exist as a discrete species in solution, such an (E·O)′ complex may have little or no lifetime as a distinct species. If $\alpha_5 = 1$, the observable KIE for this mechanism will be $KIE_{observable} = EIE_{oxocarbenium} = (\alpha_1\alpha_3)/(\alpha_2\alpha_4)$, where α_n = intrinsic KIE on step *n*. In a final step, the oxocarbenium ion undergoes nucleophilic attack by water to yield depurinated RNA and adenine.

This unique combination of equilibrium (E·O) formation followed by an isotopically insensitive step is required in order to explain the unusual experimental KIEs for this reaction, especially the 1′-^{14}C KIE (see below). This mechanism is similar to the D_N*A_N mechanism proposed for RTA-catalyzed dA-10 DNA hydrolysis.[42]

The First Step and the 1′-^{14}C KIE. The experimental value of the 1′-^{14}C KIE (0.993) distinguishes the transition state for RTA-catalyzed depurination of A-10 from all previous *N*-ribosyl transferase reactions or chemical solvolyses. The inverse KIE reflects the change in the vibrational environment of the C1′ atom between the stable reactant and its transition state. KIEs include a contribution from the reaction coordinate because one of the species involved is a transition state. The reaction coordinate is the vibrational normal mode with an imaginary frequency that corresponds to movement through the transition state either forward to products or back to reactants. The contribution to the KIE from the reaction coordinate is always normal, and in RNA depurination would be on the order of 1.01 for 1′-^{14}C. The vibrational contributions from the changes in zero point energies (ZPE) and the energies of vibrationally excited states (EXC) also contribute to the KIE.[17,43] These vibrational contributions are small for the 1′-^{14}C *equilibrium* isotope effect on forming enzyme-bound oxocarbenium ion and adenine and would be more normal for any *kinetic* isotope effect (Table 2). The calculated 1′-^{14}C EIE for the equilibrium between **1** and 3′-*endo*-**2** was 1.007 (Table 2).

Although the calculated 1′-^{14}C equilibrium isotope effect is lower than could be obtained computationally for any KIE, it is nonetheless higher than the experimental 1′-^{14}C KIE of 0.993. The result implies that the environment experienced by C1′ of the oxocarbenium ion in the active site of RTA is more constrained than the oxocarbenium ion in vacuo. Chemical precedent correlates low or inverse primary carbon isotope effects with relatively stable cationic species. An inverse EIE of 0.983 ± 0.003 was observed for the equilibrium between triphenylmethyl chloride and the triphenylmethyl cation in superacid solution.[44] As discussed by Huang et al.,[45] there is a trend toward lower primary ^{13}C KIEs of methanolysis of substituted 1-phenyl-1-bromoethanes[46] as the stability of the resulting cation increases. The lowest experimental KIE was inverse, 0.9995 for the *p*-Me compound, and correlates with the longest estimated lifetime in solution of the carbocation, 2.5×10^{-10} s.[47] This lifetime is on the order of the time scale for water diffusion[48] and suggests that this cation would have a finite existence in solution. The 1′-^{14}C EIE for formation of a more stable oxocarbenium ion, 2-deoxy-**2** from 2′-deoxy-**1**, was calculated to be 0.993, again supporting the statement that cation stability is reflected by low primary carbon isotope effects. The inverse experimental 1′-^{14}C KIE observed here suggests that the enzyme uses considerable binding energy to stabilize an oxocarbenium ion that would not otherwise have a real lifetime. The vibrational environment for that oxocarbenium ion is considerably more constrained than the unstabilized oxocarbenium ion in vacuo.

This mechanism is unique because no stable oxocarbenium ion intermediate has been previously observed for hydrolysis of a 2-hydroxy-furanoside. 2-Deoxypyranosides are more stable, and Bennet and co-workers have shown that some 2′-deoxy-glucopyranosides with cationic leaving groups form oxocarbenium ions with a borderline existence in solution, with the reactions passing through solvent-separated complexes.[49,50]

The Isotopically Insensitive Step. The requirement that the second step be isotopically insensitive implies that the rate of the second step is controlled by a nonchemical process, such as a protein conformational change or diffusion of water into position to attack the oxocarbenium ion. We represent this as a D_N*?‡A_N mechanism.[33,51] The "?‡" indicates that there is an

(40) Sims, L. B.; Lewis, D. E. *Bond order methods for calculating isotope effects in organic reactions*; Buncel, E., Lee, C. C., Eds.; Elsevier: New York, 1984; Vol. 6, pp 161−259.
(41) Parkin, D. W.; Schramm, V. L. *Biochemistry* **1987**, *26*, 913−920.
(42) Chen, X.-Y.; Berti, P. J.; Schramm, V. L. Unpublished observations.
(43) Bigeleisen, J.; Wolfsberg, M. *Adv. Chem. Phys.* **1958**, *1*, 15−76.
(44) Kresge, A. J.; Lichtin, N. N.; Rao, K. N.; Weston, R. E., Jr. *J. Am. Chem. Soc.* **1965**, *87*, 437−445.
(45) Huang, X. C.; Tanaka, K. S. E.; Bennet, A. J. *J. Am. Chem. Soc.* **1997**, *119*, 11147−11154.
(46) Bron, J.; Stothers, J. B. *Can. J. Chem.* **1969**, *47*, 2506−2509.
(47) Richard, J. P.; Rothenberg, M. E.; Jencks, W. P. *J. Am. Chem. Soc.* **1984**, *106*, 1361−1372.
(48) Kaatze, U. *J. Chem. Eng. Data* **1989**, *34*, 371−374.
(49) Zhu, J.; Bennet, A. J. *J. Am. Chem. Soc.* **1998**, *120*, 3887−3893.
(50) Huang, X.; Surry, C.; Hiebert, T.; Bennet, A. J. *J. Am. Chem. Soc.* **1995**, *117*, 10614−10621.
(51) The double dagger symbol (‡) indicates which step in the reaction is rate-limiting.

unknown, rate-limiting step between leaving group departure and nucleophilic attack by water. The asterisk indicates that the cationic intermediate has a finite lifetime, but is too short-lived to diffuse away from leaving group.[31,52] Neither an A_ND_N mechanism nor a $D_N{*}A_N$ or $D_N + A_N$ mechanism with an isotopically sensitive (i.e., chemical) second step is consistent with the experimental KIEs.

It is not possible to identify the nature of the nonchemical process in the second step of the reaction from the available data. One possibility is a protein conformational change, such as a side chain movement or a loop movement that is necessary for completion of the reaction. Protein conformational changes are often kinetically significant in enzymatic reaction mechanisms. It is also possible that the nonchemical process involves diffusion of the water nucleophile into position to attack the RTA-bound oxocarbenium ion intermediate. The ribooxocarbenium ion is too reactive to have a finite lifetime in solution, suggesting that it may form in an enzymatic environment devoid of water. The failure of RTA to form 1-methylriboside at the depurination site in the presence of solvent methanol suggests a catalytic site with restricted solvent access. Even though the oxocarbenium ion intermediate in the enzymatic complex is highly stabilized by the enzyme, it would be expected to be reactive enough to undergo nucleophilic addition with any appropriately positioned nucleophile. In this case, the rate of the second step (k_5) of the reaction would be controlled by diffusion of water into position to attack the oxocarbenium ion, a process that would not be sensitive to isotopic labels on the oxocarbenium ion.

In consideration of the inverse 1′-^{14}C experimental KIE and also in consideration of the $D_N{*}A_N$ mechanism observed for RTA-catalyzed dA-10 DNA hydrolysis,[42] a mechanism for RNA hydrolysis is proposed that is consistent with these observations. Given the inability to detect any covalent RTA-substrate intermediates,[10] transition-state stabilization must arise from noncovalent interactions.

Alternate Mechanisms Do Not Explain the Experimental KIEs. Alternate transition states considered for A-10 hydrolysis by RTA included those resulting from $D_N{*}A_N$ mechanisms with a chemical second step or an A_ND_N mechanism with strongly perturbed vibrational environments. These transition states would have to be so strongly perturbed that the contribution to the 1′-^{14}C KIE from the reaction coordinate would be dominated by the vibrational contributions. Although this possibility cannot be strictly ruled out, the transition state for a $D_N{*}?^{\ddagger}A_N$ mechanism is consistent with KIEs of Table 1 and with the mechanistic model emerging from the KIEs of hydrolysis of dA-10 DNA by RTA.[42] Therefore, the transition-state structures for both substrates are explained by a stable oxocarbenium ion intermediate. Any transition state for a A_ND_N mechanism or a $D_N{*}A_N$ mechanism with a chemical second step would have a normal contribution from the reaction coordinate frequencies. In addition, the presence of a nonzero bond order to the nucleophile and/or leaving group would cause a further normal vibrational contribution from ZPE and EXC, leading to a large, normal 1′-^{14}C KIE that would be difficult to reconcile with the experimental KIEs.

Another mechanism ruled out by the experimental KIEs is an equilibrium population of the products that can revert to substrate, with release of the products being the only irreversible step of the reaction. This would be kinetically similar to the proposed mechanism, but with k_7 being the first irreversible step and $k_6 \gg k_7$. The large, normal 1′-^{3}H KIE of 1.163 rules out this possibility. A large α-secondary KIE occurs only in species with very low leaving group and nucleophile bond orders where a significant increase in out-of-plane motions of H1′ can occur. The calculated 1′-^{3}H equilibrium isotope effect (EIE) for forming the ribosyl product is 0.997, clearly inconsistent with the experimental KIE of 1.163.

Another mechanism that was investigated was formation of a stable oxocarbenium·adenine complex with residual C1′−N9 bond order; that is, an ion·neutral complex.[53] Quantum mechanical studies have suggested that such complexes are possible between a glucopyranosyl-oxocarbenium ion and water or methanol.[54,55] Using bond order vibrational analysis[40,56] and structure interpolation[31] between reference structures **1** and (**2** + **5**), it was possible to calculate equilibrium isotope effects for formation of these hypothetical intermediates. The calculated 7-^{15}N EIEs were within experimental error at all values of C1′−N9 bond order. The calculated 9-^{15}N EIE matched the experimental KIEs within experimental error for all C1′-N9 bond orders from 0.08 to 0.42. The calculated 1′-^{14}C KIEs, however, increased with increasing C1′-N9 bond order, being in the range 1.011 to 1.021 for the range of $n_{C1'-N9}$ bond orders that matched the 9-^{15}N KIEs. Thus, the experimental KIEs are not explained by assuming an ion·neutral complex.

9-^{15}N and 7-^{15}N KIEs. The experimental primary 9-^{15}N KIE of 1.016 is smaller (less normal) than expected for full dissociation of the adenine base. Thus, the vibrational environment at both C1′ and N9 is more constrained than expected for a free oxocarbenium ion and adenine in vacuo, implying stabilization also of the dissociated adenine by the enzyme.

The large, inverse 7-^{15}N KIE of 0.981 provides evidence for protonation at that position. In solution at pH 4.0, N7 would be unprotonated.[57] Protonation at N7 by the enzyme stabilizes the formation of adenine in the (E·O) complex and results in an inverse 7-^{15}N KIE as the total bond order to N7 increases between the reactant and the transition state. The calculated EIE of 0.985 for forming the free leaving group with protonated N7 is in good agreement with the experimental KIE.

1′-^{3}H KIE. The α-secondary ^{3}H KIE of 1.163 was large and normal, consistent with an oxocarbenium ion or oxocarbenium ion-*like* species and similar to the experimental 1′-^{3}H KIEs for other *N*-riboside hydrolyses.[58−62] The calculated 1′-^{3}H KIEs were larger than those observed experimentally (Table 1). Accurate ab initio prediction of α-secondary ^{3}H KIEs is complicated by the extreme sensitivity of the value to both hyperconjugation and van der Waals interactions.[63,64] In our

(52) In an enzyme catalyzed reaction, the chemical lifetime of an intermediate may not be relevant if the leaving group is prevented from diffusing away by enzyme binding. By analogy to the X-ray crystallographic structures of nucleosidases, nucleotidases, and the structure of RTA, RNA would be expected to bind to RTA with the adenine base buried deeply in the active site cleft and the ribose ring closer to the surface. The ribooxocarbenium is not solvent exposed, since solvent methanol does not react with the intermediate. For these reasons, it is unlikely that the leaving group could diffuse away from the RNA molecule during the lifetime of the intermediate.

(53) Bowen, R. D. *Acc. Chem. Res.* **1991**, *24*, 364−371.
(54) Smith, B. J. *J. Am. Chem. Soc.* **1997**, *119*, 2699−2706.
(55) Nukada, T.; Berces, A.; Zgierski, M. Z.; Whitfield, D. M. *J. Am. Chem. Soc.* **1998**, *120*, 13291−13295.
(56) Berti, P. J. *Methods Enzymol.* **1999**, *308*, 355−397.
(57) Saenger, W. *Principles of nucleic acid structure*; Springer-Verlag: New York, 1984.
(58) Scheuring, J.; Schramm, V. L. *Biochemistry* **1997**, *36*, 8215−8223.
(59) Berti, P. J.; Blanke, S. R.; Schramm, V. L. *J. Am. Chem. Soc.* **1997**, *119*, 12079−12088.
(60) Rising, K. A.; Schramm, V. L. *J. Am. Chem. Soc.* **1997**, *119*, 27−37.
(61) Scheuring, J.; Schramm, V. L. *Biochemistry* **1997**, *36*, 4526−4534.
(62) Kline, P. C.; Schramm, V. L. *Biochemistry* **1995**, *34*, 1153−1162.
(63) Westaway, K. C. *Tetrahedron Lett.* **1975**, *48*, 4229−4232.

experience, α-secondary hydrogen KIEs are difficult to computationally reproduce with good accuracy,[65] but the value of the calculated 1′-^{3}H KIE does not influence the other calculated KIEs or change the transition state.

2′-^{3}H KIE. The *β*-secondary ^{3}H KIE of 1.012 is smaller than previously observed experimental KIEs at this position for transition states with ribooxocarbenium character.[58−62,65] Oxocarbenium ion intermediates will give rise to small 2′-^{3}H KIEs for RNA hydrolysis if the oxocarbenium ion exists in the 3′-endo ring conformation at the transition state. The ring conformation of the oxocarbenium ion is restricted to being either 3′-endo or 3′-exo by the requirement for atoms C4′−O4′−C1′−C2′ to be coplanar; a consequence of the large amount of *π*-bonding character in the O4′−C1′ bond. In the 3′-exo conformation, alignment of the C2′−H2′ bond with the vacant p-orbital of C1′ causes hyperconjugation, characterized by an increased *π*-bonding between C1′ and C2′, a lengthened C2′−H2′ bond, and 2′-^{3}H KIE similar in magnitude to the 1′-^{3}H KIE.[35,38]

Two lines of evidence support a 3′-endo conformation in the enzyme-bound oxocarbenium ion of A-10 RNA. (1) EIEs calculated for the equilibrium reaction between **1** and **2** give 2′-^{3}H EIEs of 1.178 for 3′-*exo*-**2** and 0.994 for 3′-*endo*-**2**. The latter calculated EIE is near the experimental value of 1.012. Using these calculated EIEs, along with the p-orbital−C1′−C2′−H2′ dihedral angles of 10.1° and 52.5°, respectively, and the known angular dependence of hyperconjugation,[35] we can use the experimental 2′-^{3}H KIE of 1.012 to calculate a p-orbital−C1′−C2′−H2′ dihedral angle of 48° in the enzyme-bound intermediate. This is close to the dihedral angle of 52.5° calculated in the 3′-*endo*-**2** model compound. (2) From the solution NMR[66] and a recent X-ray[67] structure of GAGA tetraloop RNAs, the adenosine residue corresponding to the scissile base adopts either a 3′-endo conformation or an unusual 2′-exo conformation. These conformations are imposed by the neighboring RNA phosphodiester backbone. Conversion between 3′-endo/2′-exo reactant conformations to a 3′-endo oxocarbenium ion requires no significant adjustment to the RNA backbone, but a 3′-exo conformation at the transition state would require large changes that would be propagated through the RNA molecule (Figure 8). Thus, the RNA tertiary structure helps explain the unusual 3′-endo conformation in the RNA transition state.

Protonation at N1 and N7. The pK_a value for N1 of a nonbase paired adenine residue is near 4.[57] The pH profile of RTA-catalyzed A-10 RNA hydrolysis is bell-shaped, with maximal activity at pH ca. 4, and with k_{cat}/K_M decreasing at increasing pH with a pH-dependence consistent with two groups with pK_a = 4.0.[11] The pH profile of RTA with its target substrate, 28 S rRNA in intact ribosomes, has not been reported but must be different from the A-10 reaction because the pH profile with small stem-loop RNA, with two ionizations in the descending limb, implies a 10^7-fold decrease in k_{cat}/K_M at the physiological pH of 7.4. A key difference between A-10 and 28 S rRNA as substrates is this pH dependence. The pH profile of A-10 RNA hydrolysis by RTA is consistent with N1 of the susceptible adenine being one of the groups with pK_a 4.0. Because this is close to the unperturbed pK_a of an adenine base, it would appear that RTA is contributing little energy to protonate the substrate at N1. In contrast, the N1 atom of A4324 in ribosomes must be protonated by the enzyme to achieve a significant catalytic rate at physiological pH. Thus, the enzyme uses binding energy from interaction with 28 S rRNA that is unavailable in interactions with A-10 RNA to promote protonation of N1 or associated groups on the enzyme.

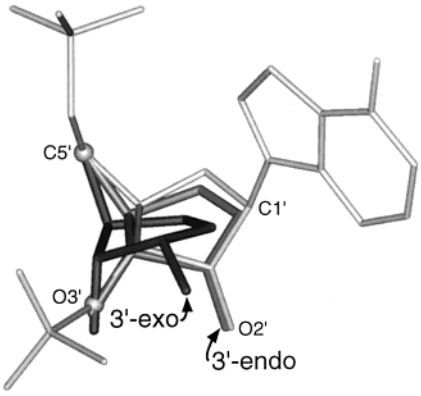

Figure 8. Oxocarbenium ion conformation. The X-ray crystallographic structure[67] of the scissile adenosine residue of the GAGA tetraloop (light gray) is superimposed with quantum mechanically optimized oxocarbenium ion structures in 3′-endo (medium gray) and 3′-exo (dark gray) conformations. The orientations of the ribosyl rings show that significant structural changes would be required to accommodate the 3′-exo conformation. Also note that the C5′ to O3′ distance in the 3′-exo model is greater by 0.5 Å, requiring further changes in the RNA backbone.

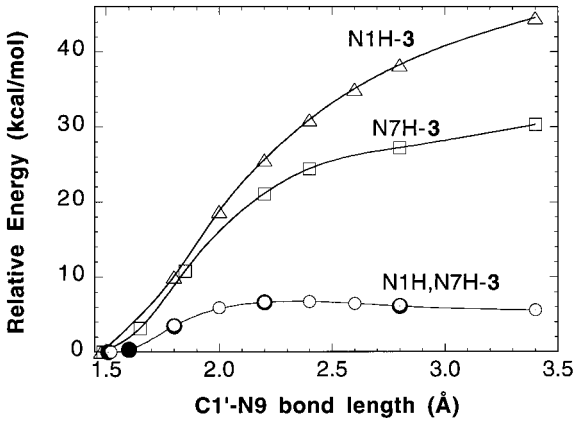

Figure 9. Energetic effects of adenine protonation on C1′−N9 bond cleavage. The energies relative to the optimized structures were calculated for increasing C1′−N9 bond lengths for different protonation states by fixing the C1′−N9 bond length at increasing values then reoptimizing the rest of the molecule and calculating the new energy. Calculations done at the RB3PW91/6-31+G**//RHF/3-21G** level of theory: (○) N1H,N7H-**3**; (□) N7H-**3**; (△) N1H-**3**. Calculations done at the RB3PW91/6-31+G**//RB3PW91/6-31+G**: (●) N1H,N7H-**3**.

The energetic importance of protonation at N1 and N7 in N-riboside hydrolysis was demonstrated by calculating the energetics of bond dissociation for compounds N1H-**3**, N7H-**3** and N1H,N7H-**3**. The energy required to break the C1′−N9 bond decreases dramatically in N1H,N7H-**3** (Figure 9). The diprotonated species, N1H,N7H-**3**, passes through a relative energetic maximum of 6.7 kcal/mol at a C1′−N9 bond length of approximately 2.4 Å. The shape of this energy profile suggests that a modest amount of enzymatic stabilization in addition to protonation would give stably dissociated substrate that could then undergo nucleophilic attack by water. In contrast, the energy of other forms of the molecule increases monotonically as the C1′−N9 distance increases up to the largest distance

(64) Poirier, R. A.; Wang, Y.; Westaway, K. C. *J. Am. Chem. Soc.* **1994**, *116*, 2526−2533.
(65) Scheuring, J.; Berti, P. J.; Schramm, V. L. *Biochemistry* **1998**, *37*, 2748−2758.
(66) Jucker, F. M.; Heus, H. A.; Yip, P. F.; Moors, E. H.; Pardi, A. *J. Mol. Biol.* **1996**, *264*, 968−980.
(67) Correll, C. C.; Munishkin, A.; Chan, Y. L.; Ren, Z.; Wool, I. G.; Steitz, T. A. *Proc. Natl. Acad. Sci. U.S.A.* **1998**, *95*, 13436−13441.

examined, 3.4 Å, and reaches final values for the fully dissociated species of 68.5 and 54.9 kcal/mol for the N1- and N7-protonated forms, respectively.

Specificity for 2′-OH. Adenosine undergoes nonenzymatic acid-catalyzed hydrolysis 650-fold more slowly than 2′-deoxyadenosine,[68] a value that is consistent with the difference between other 2′-hydroxy- and 2′-deoxynucleosides, nucleotides and *O*-glycosides[69] and for nonenzymatic, uncatalyzed *O*-glycoside hydrolysis.[70] This 650-fold difference implies a 3.8 kcal/mol higher activation energy for the 2′-hydroxy sugar. Given the structural similarity between the highly oxocarbenium ion-*like* A_ND_N transition states and the corresponding oxocarbenium ions, this difference in activation energies provides an estimate of the relative energy differences between 2-hydroxy- and 2-deoxyoxocarbenium ions. The observed 5.7-fold higher value of k_{cat}/K_M measured for RTA-catalyzed A-10 RNA substrate hydrolysis relative to the dA-10 DNA substrate indicates that RTA accelerates the reaction 3700-fold relative to that expected given the intrinsically lower reactivity of the RNA substrate. This means that the enzyme achieves 4.8 kcal/mol of stabilization of the transition state of the RNA reaction from the presence of the 2′-hydroxyl groups. Because every nucleotide residue of A-10 RNA contains a 2′-hydroxyl, it is not possible to attribute this increase in k_{cat}/K_M to a single group. However, if a significant fraction of that binding energy results from direct interaction with the 2′-hydroxyl at the depurination site, this binding energy could be used to promote catalysis. Hydrogen bonding to the 2′-hydroxyl will orient the ribosyl ring and fix it in the optimal conformation for catalysis. If the 2′-hydroxyl oxygen acts as a hydrogen bond acceptor, especially for more than one hydrogen bond, the donated hydrogens will decrease the electron withdrawing ability of the hydroxyl and thereby promote formation of the oxocarbenium ion. 2-Hydroxy-oxocarbenium ions are less stable than their 2-deoxy counterparts because the strongly electron-withdrawing 2-hydroxyl functionality destabilizes the positive charge on C1. The 4.8 kcal/mol of stabilization achieved by the enzyme, compared to the 3.8 kcal/mol intrinsically higher activation energy for RNA hydrolysis, implies that more than enough energy is derived from enzymatic interactions with the 2-hydroxyl groups to stabilize the inherently more reactive 2-hydroxy-ribooxocarbenium ion.

Enzyme Stabilization of the Intermediate. The potential interactions through the 2′-hydroxyl are only one set of many possible enzyme interactions to stabilize the oxocarbenium ion and thus promote catalysis. The substrate undergoes large changes in geometry and charge in forming the enzyme-stabilized intermediate (Figure 10). Breaking the C1′−N9 bond changes the relative disposition of the ribosyl ring and the adenine ring. The geometry of the ribosyl ring changes, with the ring becoming planar and the C1′−O4′ and the C1′−C2′ bonds becoming shorter in the oxocarbenium ion. There is positive charge on the oxocarbenium ion, and protonation of the adenine ring at two sites also changes the distribution of charge. These changes in geometry and charge could be exploited by the enzyme to stabilize the (E·O) complex.

Significance of the RTA·A-10 Transition State. Stereoelectronic effects dominate transition states in solution, where molecules are free to adopt the most energetically favorable conformations. In the constrained geometry of the RNA phosphodiester backbone, the energetics of base-pairing exceed those of geometric rearrangement for the most favorable stereoelectronic interactions. The transition-state geometry is established by the enzymatic forces leading to adenine departure with constrained ribooxocarbenium geometry. The constraints generate a cationic intermediate with a longer life than expected in solution.

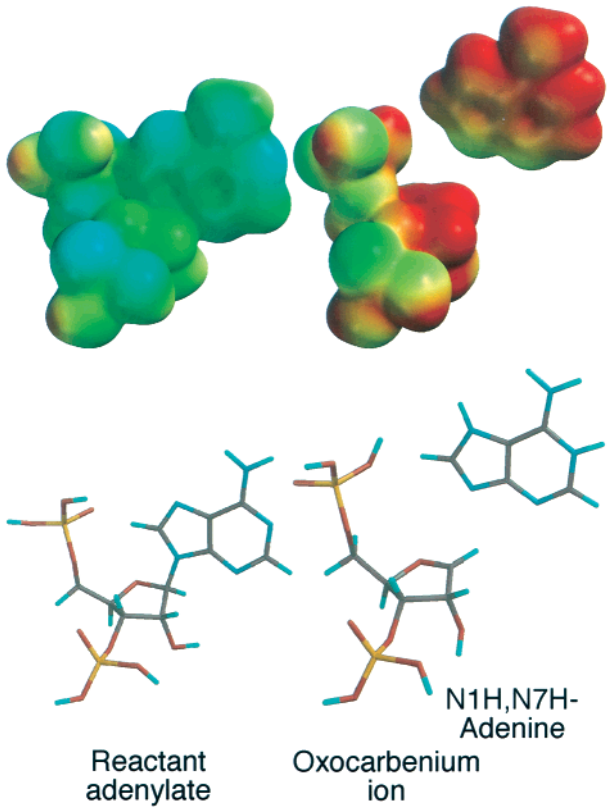

Figure 10. Structures and charge distribution of the reactant adenylate and (oxocarbenium ion + adenine) intermediate. Electrostatic potentials are projected onto the molecular surfaces of the molecules, with red representing positive electrostatic potential and blue representing negative potential. Stick figures in the same orientation are shown below the structures. (Left) structure of A15 of the X-ray crystal structure of a GAGA tetraloop.[67] (Right) ribooxocarbenium ion and N1H,N7H-adenine. The oxocarbenium ion is derived from computationally optimized 3′-*endo*-**2**, with the phosphate side chains taken directly from the X-ray structure. The N1H,N7H-adenine is computationally optimized **4**.

This study demonstrates that KIE studies can provide detailed mechanistic and structural information on the transition state of large systems exemplified by the RNA substrate. The enzymatic contacts responsible for catalysis are yet to be revealed; however, knowledge of the transition-state structure provides the information needed for design of transition-state inhibitors. It is anticipated that complexes of RTA with a transition-state inhibitor will elucidate details of the chemical mechanism that lead to the unusual ribooxocarbenium ion species at the transition state.

Supporting Information Available: *Z*-matrixes of the optimized structures of compounds **1**−**5** are available in ASCII and PDF format. This material is available free of charge via the Internet at http://pubs.acs.org.

JA992750I

(68) Venner, H. Z. *Physiol. Chem.* **1964**, *339*, 14−27.
(69) Capon, B. *Chem. Rev.* **1969**, *69*, 407−498.
(70) Wolfenden, R.; Lu, X.; Young, G. *J. Am. Chem. Soc.* **1998**, *120*, 6814−6815.